

1 **Interactive network configuration maintains bacterioplankton**
2 **community structure under elevated CO₂ in a eutrophic coastal**
3 **mesocosm experiment**

4

5 Xin Lin^{†*1}, Ruiping Huang^{†1}, Yan Li¹, Futian Li¹, Yaping Wu^{1,2}, David A. Hutchins³,
6 Minhan Dai¹, Kunshan Gao^{*1}

7

8 **Institutions:**

9 ¹ State Key Laboratory of Marine Environmental Science, College of Ocean & Earth Sciences, Xiamen
10 University, Xiamen 361102, PR China.

11 ²College of Oceanography, Hohai University, No.1 Xikang road, Nanjing 210000, China.

12 ³Department of Biological Sciences, University of Southern California, 3616 Trousdale Parkway, AHF
13 301, Los Angeles, CA 90089-0371, USA.

14

15 [†] These authors contributed equally to this work.

16 *Correspondence to:* Xin Lin (xinlinulm@xmu.edu.cn, TEL: +865922880171);

17 Kunshan Gao (ksgao@xmu.edu.cn, TEL: +865922187963)

18

19

20

21

22

23

24

25

26

27

28

29

30

31

32

1 **Abstract**

2 There is increasing concern about the effects of ocean acidification on marine biogeochemical and
3 ecological processes and the organisms that drive them, including marine bacteria. Here, we examine the
4 effects of elevated CO₂ on the bacterioplankton community during a mesocosm experiment using an
5 artificial phytoplankton community in subtropical, eutrophic coastal waters of Xiamen, Southern China.
6 Through sequencing the bacterial 16S rRNA gene V3-V4 region, we found that the bacterioplankton
7 community in this subtropical, high nutrient coastal environment was relatively resilient to changes in
8 seawater carbonate chemistry. Based on comparative ecological network analysis, we found that
9 elevated CO₂ hardly altered the network structure of high abundance bacterioplankton taxa, but appeared
10 to reassemble the community network of low abundance taxa. This led to relatively high resilience of the
11 whole bacterioplankton community to the elevated CO₂ level and associated chemical changes. We also
12 observed that the Flavobacteria group, which plays an important role in the microbial carbon pump,
13 showed higher relative abundance under the elevated CO₂ condition during the early stage of the
14 phytoplankton bloom in the mesocosms. Our results provide new insights into how elevated CO₂ may
15 influence bacterioplankton community structure.

16

17

18 **Key words:** elevated CO₂; mesocosm; bacterioplankton community; ecological network; Flavobacteria

19

1 **1 Introduction**

2 It is well established that ocean acidification is being caused by increased uptake of
3 anthropogenically-derived carbon dioxide in the surface ocean. Consequently, it is predicted that under a
4 “business-as-usual” CO₂ emission scenario, the present average surface pH value will drop 0.4 units over
5 the next century (Gattuso et al., 2015). Despite a growing interest in the importance of the roles of marine
6 bacterioplankton in ocean ecosystems and biogeochemical cycles, our current understanding of their
7 responses to ocean acidification is still limited. Over half of autotrophically-fixed oceanic CO₂ is
8 processed by heterotrophic bacteria and archaea through the microbial loop and carbon pump (Azam,
9 1998; Jiao et al., 2010). Furthermore, marine bacterioplankton play an essential role in marine
10 ecosystems and global biogeochemical cycles central to the biological chemistry of Earth (Falkowski et
11 al., 2008). The null hypothesis is that elevated CO₂ will not affect biogeochemical processes (Liu et al.,
12 2010; Joint et al., 2011), however more investigation is required. Ocean acidification mesocosm
13 experiments provide good opportunities to explore the responses of marine bacteria to elevated CO₂.
14 Mesocosm studies conducted in the Arctic Ocean, Norway, Sweden and the coastal Mediterranean Sea
15 using natural phytoplankton communities have often found that elevated CO₂ has little direct effect on
16 the bacterioplankton community (Zhang et al., 2013; Ray et al., 2012, Roy et al., 2013; Baltar et al.,
17 2015). In contrast, phytoplankton blooms induced by high CO₂ can sometimes have significant indirect
18 effects on heterotrophic microbes, thus altering bacterioplankton community structure (Allgaier et al.,
19 2008, Hutchins and Fu, 2017).

20 Although most mesocosm studies have showed that elevated CO₂ had an insignificant impact on
21 bacterioplankton community structure, microcosm experiments have demonstrated that small changes in
22 pH can have direct effects on marine bacterial community composition (Krause et al., 2012). Ocean

1 acidification experiments using natural biofilms showed bacterial community shifts, with decreasing
2 relative abundance of Alphaproteobacteria and increasing relative abundance of Flavobacteriales (Witt et
3 al., 2011). Coastal microbial biofilms grown at high CO₂ level also showed different community
4 structures compared to those grown at ambient CO₂ level in a natural carbon dioxide vent ecosystem
5 (Lidbury et al., 2012). Ocean acidification also affects the community structure of bacteria associated
6 with corals. It has been reported that the relative abundance of bacteria associated with diseased and
7 stressed corals increased under decreasing pH conditions (Meron et al., 2011). A very limited number of
8 studies focused on the effects of ocean acidification on isolated bacterial strains have also been
9 reported. Under lab conditions, growth of *Vibrio alginolyticus*, a species belonging to the class
10 Gammaproteobacteria, was suppressed at low CO₂ levels (Labare et al., 2010). In contrast, stimulation of
11 growth was observed for one Flavobacteria species under high CO₂ levels (Teira et al., 2012).

12 Taken together, results from mesocosm, microcosm and cultured isolate experiments indicate a
13 potentially complex interaction between different groups of marine bacteria in response to elevated CO₂.
14 One promising method to elucidate these types of complex interactions is network analysis. Ecological
15 network approaches have been successfully applied to investigate the complexity of interactions among
16 zooplankton and phytoplankton from different trophic levels during the Tara Oceans Expedition project
17 (Lima-mendez et al., 2015; Guidi et al., 2015). Elucidating the complex interactions between
18 bacterioplankton and other marine organisms under anthropogenic perturbations will increase our
19 understanding of their impact in a holistic way. Previous studies using ecological network analysis
20 showed that elevated CO₂ significantly impacted soil bacterial/archaeal community networks, by
21 decreasing the connections for dominant fungal species and reassembling unrelated fungal species in a
22 grassland ecosystem (Tu et al., 2015). It was also reported using ecological network analysis that

1 elevated $p\text{CO}_2$ did not significantly affect microbial community structure and succession in the Arctic
2 Ocean, suggesting bacterioplankton community resilience to elevated $p\text{CO}_2$ (Wang et al., 2016).

3 It has been reported that eutrophication problems in coastal regions lead to complex cross-linkages
4 between ocean acidification and eutrophication (Cai et al., 2011). The occurrence of ocean acidification
5 combined with other environmental stressors such as eutrophication can potentially produce synergistic
6 or antagonistic effects on bacterioplankton that differ from those caused by ocean acidification alone.
7 Although there are some reports from mesocosm experiments describing the response of bacteria to
8 elevated CO_2 , there are limited studies on how the bacterial community responds to ocean acidification in
9 eutrophic marine environments. In this study, Illumina sequencing of the V3-V4 region of the bacterial
10 16S rRNA gene was used to explore the effects of ocean acidification on bacterioplankton community
11 composition and ecological network structure in a eutrophic coastal mesocosm experiment.

12 **2 Methods**

13 **2.1 Mesocosm setup and carbonate system manipulation**

14 The mesocosm experiment was conducted in the FOANIC-XMU (Facility for the Study of Ocean
15 Acidification Impacts of Xiamen University) mesocosm platform located in Wuyuan Bay, Xiamen,
16 Fujian province, East China Sea (N24°31'48", E118°10'47") during the months of December 2014 and
17 January 2015 (Fig. S1). Each transparent thermoplastic polyurethane (TPU) cylindrical mesocosm bag
18 was 3 m deep and 1.5 m wide (~4000 L total volume). After setting up the mesocosm bags within steel
19 frames, in situ seawater from Wuyuan Bay was filtered through a 0.01 μm water purifying system and
20 used to simultaneously fill eight bags within 24 hours. The initial in situ seawater $p\text{CO}_2$ in Wuyuan Bay
21 was ~650 μatm , due to the active decomposition of land-sourced organic compounds. In order to reach
22 the target low $p\text{CO}_2$ associated with ambient air (400 ppm), Na_2CO_3 was added to each mesocosm to

1 increase dissolved inorganic carbon (DIC) and total alkalinity (TA) by 100 $\mu\text{mol/L}$ and 200 $\mu\text{mol/L}$
2 respectively, based on carbonate system calculations (Lewis and Wallace, 1998). To adjust seawater to
3 projected end of this century seawater conditions of ~ 1000 ppm CO_2 , about 5 L of CO_2 saturated filtered
4 seawater was added to 4 mesocosms (#2, #4, #7, #9), collectively considered to be the HC treatment,
5 while the other 4 mesocosms (#1, #3, #6, #8) were considered to be the LC treatment. Throughout the
6 experiment, HC mesocosms and LC mesocosms were bubbled with air containing 1000 ppm and 400
7 ppm CO_2 , respectively supplied by CO_2 Enrichlors (CE-100B, Wuhan Ruihua Instrument & Equipment
8 Ltd, China) at a flow rate of 4.8 L per minute. Two diatoms, *Phaeodactylum tricornutum* CCMA 106
9 from the Centre for Collections of Marine Bacteria and Phytoplankton of the State Key Laboratory of
10 Marine Environmental Science (Xiamen University, China), and *Thalassiosira weissflogii* CCMP 102
11 from the Provasoli-Guillard National Center for Culture of Marine Phytoplankton (CCMP, USA), as well
12 as the coccolithophorid *Emiliana huxleyi* CS-369 from the Commonwealth Scientific and Industrial
13 Research Organization (CSIRO, Australia) were used as inoculum to construct a model phytoplankton
14 community. The effects of ocean acidification on these phytoplankton species mentioned above have
15 been intensively studied in the lab at physiological, biochemical and molecular levels. However, it is
16 difficult to extrapolate the response of these species to ocean acidification in natural complex
17 environments based on laboratory single species experiments (Busch et al., 2015). Our experiment was
18 designed as an intermediary step between laboratory and natural community field experiments, with
19 isolates of non-axenic phytoplankton being added to filtered natural waters. In this way, we were able to
20 investigate the effect of OA on phytoplankton and bacterioplankton in naturally eutrophic waters while
21 minimizing the complexity of shifting compositions of natural phytoplankton communities. Correlated
22 data about the effects of ocean acidification on the artificial phytoplankton community using the same

1 mesocosm system are available in (Jin et al., 2015) and (Liu et al., 2017).

2 The initial concentration of both *P. tricornutum* and *T. weissflogii* was 10 cells/mL, and *E. huxleyi* was
3 added at 20 cells/mL. The phytoplankton cultures were not axenic. The bacteria community
4 composition in the inoculated phytoplankton culture is shown in Fig. S2. Bacteria were not detectable
5 by flow cytometry in the filtered seawater just before inoculation. The three species of non-axenic
6 phytoplankton with bacterioplankton were mixed and then inoculated into each mesocosm bag. Thus, we
7 considered the initial bacterioplankton community to be the same or similar in each mesocosm bag
8 because the phytoplankton culture with bacterioplankton were evenly distributed into each mesocosm
9 bag for inoculation. The mesocosm and the CO₂ bubbling system were not sterile and not completely
10 closed during the experiment. Therefore, [natural bacterioplankton were undoubtedly introduced into the](#)
11 [mesocosm system through aeration and air-sea exchange](#), and the bacterioplankton community in this
12 mesocosm experiment was derived from both the bacteria added with the inoculated phytoplankton
13 culture, and the natural local prokaryotic assemblage.

14 The use of the natural phytoplankton and bacterioplankton communities in this mesocosm experiment
15 would better represent the effects of ocean acidification on natural phytoplankton and bacterioplankton
16 communities. However, considering the highly eutrophic in situ seawater in Wuyuan Bay, it was
17 impractical to use the in situ seawater with the in situ natural community (bacterioplankton,
18 phytoplankton, zooplankton) directly without filtration, because of the dense phytoplankton bloom that
19 could be induced within several days, making the *p*CO₂ very difficult to keep under control. Alternatively,
20 we would have had to dilute 4 tons of seawater in the mesocosm bags at least every two days to maintain
21 the cell density and CO₂ concentration. Furthermore, considering a number of studies on the typical
22 phytoplankton responses to OA that have been carried out in laboratory, it was indeed a natural

1 progression for us to use typical model phytoplankton species to initiate the mesocosm studies before
2 using natural communities. Therefore, using the filtered seawater with inoculated isolates was reasonable
3 and logistically practical for our experiment.

4 **2.2 Bacteria sampling, filtration and sample selection**

5 A total of 500 mL to 2 L of water, depending on bacterial concentration, was collected from the
6 mesocosms. Six of the mesocosms (HC: #2, #4, #7 and LC: #1, #6, #8) were chosen for further study.
7 The inter-replicate variation in mesocosm experiments is usually more significant than in lab
8 experiments, because mesocosm experiments are conducted in open environments. Initially we had 4
9 replicates for each treatment, however, mesocosm bag 9 had a hole and mesocosm bag 3 was
10 contaminated by other phytoplankton in the beginning. Therefore, we did not consider the data from
11 these two compromised bags. Furthermore, three replicates of each treatment in our experiment to some
12 extent balanced out the bacteria introduction contingency, although the inter-replicate variation was
13 significant. Samples from days 4, 6, 8, 10, 13, 19, and 29 were collected in this study due to time,
14 personnel and equipment constraints. Sequential size fractionated filtration (2 μm and 0.2 μm
15 polycarbonate filters) by peristaltic pump was used to filter seawater collected from the mesocosm bags.
16 We tried to do sampling at day 2, but the samples were not successfully collected, probably due to very
17 high concentration of TEP (Transparent Exopolymer Particles) which easily blocked the polycarbonate
18 filter. Some replicates were missing at day 4 because we were able to successfully extract enough DNA
19 for sequencing only from bag 1, bag 7 and bag 6, also probably due to high TEP at day 4. It has been
20 reported that high TEP concentration was associated with high bacteria biomass (Sugimoto et al.,
21 2007, Ramaiah et al., 2000). According to the bacterioplankton abundance data (Fig. S3, Yibin Huang
22 et al.), the average bacterioplankton abundance was 6.69×10^9 cells/ml and 9.71×10^9 cells/ml at day 2

1 and day 4 respectively.

2 **2.3 DNA extraction, 16S rDNA V3-V4 region amplification and Illumina MiSeq sequencing**

3 Samples collected by 0.2 µm polycarbonate filters as described above were washed with PBS buffer and
4 then centrifuged at 9600g to obtain a cell pellet. A previously described DNA extraction protocol
5 (Francis et al., 2005) was utilized with some modifications, using the columns for DNA purification
6 from a bacteria DNA extraction kit (Tiangen DP302, China). Amplification, library construction and
7 sequencing were performed offsite at ANNOROAD using the DNA samples isolated as described above.

8 Primers were 341F (5'-CCTACGGGNGGCWGCAG-3') and 805R
9 (5'-GACTACHVGGGTATCTAATCC-3'), targeting the V3-V4 hyper variable regions of bacterial 16S
10 rRNA gene. The PCR amplification condition was as follows: initial denaturation at 95°C for 3 min, 25
11 cycles of denaturation at 95°C for 30 s, annealing at 55°C for 30 s and extension at 72°C for 30 s, then
12 final extension at 72°C for 5 min. DNA library construction and sequencing followed the MiSeq Reagent
13 Kit Preparation Guide (Illumina, USA).

14 **2.4 Sequence assignment and sequence statistics analysis**

15 Clean paired-end reads were merged using PEAR (Zhang et al., 2014). The remaining raw sequences
16 were distinguished and sorted by unique sample tags. Unique operational taxonomic units (OTUs) were
17 picked against Greengenes database (http://greengenes.lbl.gov/cgi-bin/JD_Tutorial/nph-16S.cgi)
18 (McDonald et al., 2012) at 97% identity. OTUs with less than 2 reads were not considered. According to
19 the reference database, the representative sequences for each OTU were aligned using PyNAST
20 (Caporaso et al., 2010a). Finally, the phylogenetic tree was generated from the Graphlan (Langille
21 et al., 2013) using information on both the relative abundance and phylogenetic relationship of
22 observed species. QIIME 1.8.0 was used for sequence analysis including OTUs extraction for

1 bacterioplankton community structure analysis, OTUs overlapping analysis, species diversity, species
2 richness analysis and Principal Components Analysis (PCA) (Caporaso et al., 2010b). Bacterioplankton
3 community composition differences were assessed by Unweighted UniFrac distance using QIIME 1.8.0
4 as well. Dissimilarity tests were based on the Bray-Curtis dissimilarity index using analysis of
5 similarities (ANOSIM) (Clarke, 1993), non-parametric multivariate analysis of variance (ADONIS)
6 (Anderson, 2001), and multi-response permutation procedures (MRPP) (Mielke et al., 1981). Observed
7 species, Chao index, Shannon index and Simpson index were used for estimating the community
8 diversity. Analysis of variance (ANOVA) followed by T-test was performed to determine any significant
9 differences between HC and LC treatments.

10 **2.5 Ecological network construction and analysis**

11 As previously described, ecological network construction and analyses were performed based on the
12 relative abundance of OTUs in HC and LC treatments with three biological replicates
13 (<http://129.15.40.240/mena/>, Wang et al., 2016). The sequencing data from each mesocosm bag with
14 time series throughout the experiment were considered as different replicates. First, the similarity
15 matrices of the relative abundance of OTUs in LC and HC conditions were created respectively using
16 Pearson correlation coefficient across time points with biological replicates by a random matrix theory
17 (RMT)-based approach. Cut-off values were determined according to R^2 of power-law larger than 0.8
18 and equal between two manipulations to construct network structure. In order to ensure the constructed
19 networks were not random, biologically meaningless networks, 100 networks from the same matrix were
20 constructed and randomized. This resulted in the experimental networks being different from random
21 networks judging by significantly higher modularity, clustering coefficient and geodesic distance (Table
22 1). Then, module separation was produced using greedy modularity optimization, and $Z-P$ values for all

1 nodes were calculated. In addition, to compare networks, the network connection was randomly rewired
2 and network topological properties were calculated. Finally, the bacteria network interaction was
3 visualized by Cytoscape v.3.3.0. The Z - P plots were constructed based on within-module (Z) and
4 among-module (P) values of each node derived from ecological network analysis. Ecological network
5 analysis is a novel RMT-based framework for studying microbial interactions. A node in ecological
6 network analysis shows an OTU and a link demonstrates a connection between two OTUs. The shortest
7 path between nodes is indicated by geodesic distance. Since the network constructed by OTUs can be
8 separated into several sub-communities, or modules, the modularity value indicates how well a network
9 can be divided into different sub-communities. Clustering coefficients demonstrate how well an OTU is
10 connected with other OTUs, while average clustering coefficients indicate the extent of connection in a
11 network.

12 **3 Results**

13 **3.1 Environmental parameters and experimental timeline**

14 The initial inorganic nitrogen, PO_4^{3-} , and SiO_3^{2-} concentrations were 70–75 $\mu\text{mol/L}$, 2.5–2.6 $\mu\text{mol/L}$, and
15 38–39 $\mu\text{mol/L}$, respectively. Except for SiO_3^{2-} , nutrient concentrations decreased with rapid growth of
16 the phytoplankton and reached low concentrations by day 15. The dissolved total inorganic nitrogen
17 dropped from an initial concentration of $74.9 \pm 2.87 \mu\text{mol/L}$ to $57.2 \pm 4.37 \mu\text{mol/L}$ in the HC condition
18 and $72 \pm 5.90 \mu\text{mol/L}$ to $53.6 \pm 5.60 \mu\text{mol/L}$ in the LC condition by day 8, and reached low
19 concentrations by day 15 (average $3 \mu\text{mol/L}$ in LC and average $6 \mu\text{mol/L}$ in HC).

20 pH_{NBS} was determined on the scene with a pH/mV/ORP Meter (LEAN) calibrated with National
21 Bureau of Standards (NBS) buffers. Samples for DIC measurement were collected into 250 ml brown
22 borosilicate glass bottles and poisoned with 250 μL saturated HgCl_2 solution. DIC was determined by

1 acidification of 0.5 mL samples and subsequently infrared quantification of CO₂ with an Apollo® DIC
2 Analyzer. pH_{total} was determined using a Orion 3 Star pH Benchtop analyzer and a Orion Ross
3 combined pH electrode, which was calibrated against three NIST-traceable pH buffers (pH 4.01, 7.00
4 and 10.01) (Cao et al. 2011). The pCO₂ and TA values in this study were calculated from DIC and
5 pH_{total} by the CO2SYS Program (Lewis and Wallace, 1998). The carbonate chemistry data at different
6 time points are shown in Table S1. A comprehensive description of carbonate chemistry measurements
7 and analysis during this mesocosm experiment is given in (Yan Li et al, unpublished). The initial pCO₂
8 of 373.0 ± 43.9 µatm (pH_{NBS}: 8.18 ± 0.02) in the LC treatment and 1296.0 ± 159.6 µatm (pH_{NBS}: 7.75 ±
9 0.04) in the HC treatment increased and reached a peak value of 922.5 ± 142.0 µatm (pH_{NBS}: 7.74 ± 0.08)
10 in the LC treatment at day 8 and 1879.6 ± 145.4 µatm (pH_{NBS}: 7.49 ± 0.05) in the HC treatment at day 4.
11 After reaching the peak, the pCO₂ values of both treatments decreased and were no longer statistically
12 different from day 13 onwards due to rapid CO₂ uptake by the phytoplankton, despite air containing 1000
13 ppm CO₂ being continuously bubbled into the HC treatments (Fig. 1 a, b). The bacterioplankton biomass
14 were very high on day 2 and day 4 (Fig. S3). However, the large amount of DIC (dissolved inorganic
15 carbon) produced by this high biomass of bacterioplankton could not be consumed by the phytoplankton
16 which were still at very low biomass, thus explaining the significant DIC production in the beginning.
17 The continuous rise of pCO₂ until the phytoplankton reached a certain concentration in the beginning was
18 also due to the high concentration of bacteria and the low concentration of phytoplankton, even though
19 the seawater was being aerated at target pCO₂. *P. tricornutum* and *T. weissflogii* were the dominant
20 species throughout the whole phytoplankton bloom in both HC and LC conditions. Chlorophyll *a* (Chl*a*)
21 concentration and diatom cell densities were used to identify changes in the diatom bloom following
22 inoculation (Fig. 1c, Liu et al., 2017). Chl*a* concentration increased from 0.23 ± 0.12 µg/L to 5.33 ± 1.82

1 $\mu\text{g/L}$ in the LC conditions, and from $0.19 \pm 0.07 \mu\text{g/L}$ to $5.75 \pm 1.17 \mu\text{g/L}$ in the HC conditions from day
2 4 to day 9. Thereafter, *Chla* concentration increased significantly and peaked at $109.9 \pm 38.04 \mu\text{g/L}$ in the
3 LC treatment and $108.6 \pm 46.07 \mu\text{g/L}$ in the HC treatment at day 15. Subsequently, *Chla* concentrations
4 in both treatments were maintained at high concentrations until day 25 and decreased progressively
5 afterward. The bloom process identified by cell concentration of *P. tricornutum* and *T. weissflogii* was
6 similar with that illustrated by *Chla* concentration. The growth of these two diatom species entered into
7 logarithmic phase from day 2. Cell density reached highest concentration at day 15 and day 19 for *T.*
8 *weissflogii* and *P. tricornutum* respectively, and then dropped down slowly. The coccolithophore
9 *Emiliania huxleyi* largely disappeared from the experimental mesocosms. A comprehensive description
10 of phytoplankton cell density, *Chla* concentration, particle organic carbon (POC) and particle organic
11 nitrogen (PON) during the experiment is given in (Liu et al., 2017).

12 **3.2 Overview of sequencing analysis**

13 Following sequencing, 828524 high quality sequences were kept after processing (Table. S2), and 39.3%
14 of assembled reads were successfully aligned with the database. As a result, a total of unique 557
15 OTUs were generated after clustering at a 97% similarity level. 49.1% of OTUs were classified to
16 genera level with high taxonomic resolution (Table. S3). The phylogenetic tree was constructed based on
17 the sequences derived from all of the samples (Fig. S4). The bacterioplankton from all of the samples in
18 this study were identified as members of Bacteriodetes or Proteobacteria phylums. The most dominant
19 OTUs were Alphaproteobacteria, Rhodobacterales, Rhodobacterceae and Sediminicola at class, order,
20 family and genus level respectively (Fig. S5). The most abundant sequences at class, order, family and
21 genus levels accounted for 43.4 %, 42.6 %, 41.7% and 32.8 % of all sequences respectively.

1 **3.3 Bacterioplankton community structure throughout the phytoplankton bloom**

2 The bacterioplankton community structure in the mesocosm bags was very different from that in the
3 originally inoculated phytoplankton cultures by day 4. For instance, some bacterioplankton phyla not
4 detected in the original phytoplankton culture were observed in the samples collected on day 4. This
5 may indicate that the bacterioplankton from the natural environment gradually became dominant in the
6 mesocosm bags from day 0 to day 4. For example, Epsilonbacteria appeared in the mesocosms at day 4,
7 while no Epsilonbacteria were detected in the coccolithophore or diatom cultures. Nearly 50% of the
8 bacterioplankton in the mesocosms were composed of Epsilonbacteria in D4.1 (Fig. S2, Fig. 2).

9 Bacterioplankton community structure underwent dynamic changes during the diatom bloom in both
10 the HC and LC treatments, varying significantly at different stages of the phytoplankton bloom (Fig. 2).
11 At the phylum level, the bacterioplankton were dominated by Proteobacteria, while the relative
12 abundance of Bacteroidetes was very low when nutrients were replete and diatom biomass was not high.
13 However, Bacteroidetes increased dramatically as diatom biomass increased, and began to drop down
14 after reaching a peak at day 10 (Fig. 2 and Fig. 3). In contrast, Proteobacteria began to increase after
15 reaching their lowest concentration at day 10.

16 The Alphaproteobacteria, Flavobacteria, and Gammaproteobacteria classes with high abundance in all
17 samples were selected for further analysis. The proportion of the Gammaproteobacteria class from the
18 Proteobacteria phylum was very high at the beginning of the experiment (50.2 ± 13.8 % in the HC
19 treatment and 44.1 ± 6.4 % in the LC treatment at day 6) and decreased throughout the duration of the
20 experiment. On the other hand, the Alphaproteobacteria class, also from the Proteobacteria phylum,
21 decreased from initially high proportions (46.9 ± 13.2 % in the HC treatment and 43.9 ± 11.6 % in the LC
22 treatment) at day 6 to low proportions at day 10 (27.2 ± 2.8 %) in the HC treatment, but remained almost

1 unchanged (44.6 ± 7.5 %) in the LC treatment and increased to 63.2 ± 27.3 % in the HC treatment and
2 60.8 ± 32.7 % in the LC treatment at day 29 (Fig. 2 and Fig. 3). The relative abundance of the
3 Flavobacteria class from the Bacteroidetes increased from the beginning and reached a peak at day 10
4 (52.2 ± 4.2 % in the HC treatment and 24.8 ± 16.9 % in the LC treatment), then dropped down until day
5 19 (19.9 ± 2.2 % in the HC treatment and 18.0 ± 15.4 % in the LC treatment) (Fig. 2 and Fig. 3). The
6 proportional variation of the Flavobacteriales order and the Rhodobacterales order showed similar trends
7 with the Flavobacteria class and the Alphaproteobacteria class, respectively, as shown in Fig. 2 and Fig.
8 3.

9 **3.4 The effects of elevated CO₂ on bacterioplankton community structure**

10 Bacterial community structures of the HC and LC treatments were compared at different sampling
11 time-points (Fig 2), and a dissimilarity test based on ANOSIM, MRPP and ADONIS methods showed
12 that no statistically significant differences were observed (Table 2). PCA analysis also agreed with the
13 dissimilarity test (Fig. S8). The bacterioplankton community diversity in all samples was estimated by
14 observed species, Chao index, Shannon index and Simpson index. Rarefaction curves showed no
15 remarkable differences in community diversity between HC and LC, regardless of the time point (Fig.
16 S6). In general, bacterioplankton community diversity in both HC and LC treatments followed the same
17 trend, in that it peaked at day 10 and declined for the remainder of the experiment (Fig. S7).

18 Although the general trend of bacterioplankton community structure variation was similar in both the
19 HC and LC treatments as described above, some groups of bacterioplankton showed different responses
20 to elevated CO₂ at some time points. Notably, Bacteroidetes (predominantly Flavobacteria) had a higher
21 average proportion in the HC treatment (52.2 % of Bacteroidetes and 52.2 % of Flavobacteria) than in the
22 LC treatment (25.2 % Bacteroidetes and 24.8 % Flavobacteria) at the early stage of the diatom bloom at

1 day 10 ($p=0.049$ and 0.053 respectively). In contrast Proteobacteria, especially the Alphaproteobacteria,
2 were observed to have lower proportion in the HC treatment (47.8 % of Proteobacteria and 27.2% of
3 Alphaproteobacteria) than in the LC treatment (74.8 % of Proteobacteria and 44.6% of
4 Alphaproteobacteria) at day 10 ($p=0.049$ and 0.019 respectively, Fig. 3). At a higher taxonomic level,
5 Flavobacteriales demonstrated higher relative abundance in the HC treatment (52.2 %) compared to the
6 LC treatment (24.8 %) at day 10 ($p=0.053$), while for Rhodobacterales the inverse pattern was observed
7 ($p=0.020$). Moreover, Flavobacteriaceae were observed to have a relatively higher ratio in the HC
8 treatment (50.3 %) compared to the LC treatment (24.0 %) at day 10 ($p=0.053$), whereas
9 Rhodobacteraceae demonstrated the opposite pattern ($p=0.021$, Fig. 3). It is notable that
10 Alteromonadales, belonging to the Gammaproteobacteria, had a higher ratio in the HC treatment
11 compared to the LC treatment at day 19 and day 29, although this was not statistically significant ($p=0.24$
12 and 0.34 at day 19 and 29 respectively).

13 **3.5 The effects of elevated CO₂ on bacterioplankton community interactions**

14 Both HC and LC networks were dominated by Alphaproteobacteria, Gammaproteobacteria and
15 Flavobacteria, suggesting their vital roles in maintaining stability of microbial ecosystems under both
16 HC and LC conditions. The observation of more negative links compared to positive links indicates the
17 dominant relationship among bacterioplankton is competitive rather than mutualistic under both the HC
18 and LC treatments. The average connectivity and clustering coefficient of the network were higher in the
19 HC treatment than in the LC treatment, while geodesic distance and modularity value was higher in the
20 the LC treatment. Bacterioplankton formed more modules under the LC treatment, but were densely
21 connected in less modules under the HC treatment (Table 1, Fig. 4). However, as shown in Fig. 4, the
22 links among the OTUs with high abundance, 558885 (Rhodobacteraceae), 572670 (Rhodobacteraceae),

1 190052 (Flavobacteriaceae), 107130 (Flavobacteriaceae) and 4331023 (Rhodobacteraceae), were
2 positive in both HC and LC.

3 Interestingly, some nodes that were sparsely distributed in independent modules in the LC network
4 formed dense modules with high connectivity in the HC network (Fig. 4). As the OTUs connected within
5 a module, they could be considered as a putative bacterioplankton ecological niche (Zhou et al., 2010). It
6 is plausible that elevated CO₂ disrupted the connection between different bacterioplankton community
7 niches, but enhanced alternative connections among species within certain ecological niches. Within
8 module connectivity (*Zi*) and among-module connectivity (*Pi*) indexes were used to identify key module
9 members (Olesen et al., 2007, Fig. 5). In an ecological context, the peripherals may represent specialists,
10 while module hubs and connectors may be considered more as intra-module and inter-module generalists
11 respectively. Network hubs are usually considered as super-generalists (Deng et al., 2012). It is
12 interesting that the numbers of connectors that are considered as generalists were reduced, whereas
13 module hubs were increased under the HC treatment. However, two network hubs, the super-generalists
14 that are more important than module hubs and connectors, were detected in the LC network but not in the
15 HC network (Fig. 5).

16 **4 Discussion**

17 This study was designed to bridge the gap between lab cultures and field studies, with isolates of
18 non-axenic phytoplankton being added to filtered natural waters. The lab conditions possibly have
19 selected for a fast-growing bacterial community adapted to live with semi-continuous phytoplankton
20 culture. Therefore, the inoculated bacterioplankton were likely preconditioned to lab conditions in
21 semi-continuous phytoplankton cultures prior to the experiment. However, the bacterioplankton from
22 the natural environment gradually became dominant in the mesocosm bags from day 0 to day 4, based

1 on the comparison of the community at day 4 and the original community in the phytoplankton cultures.
2 For instance, during these 4 days members of the *Arcobacter* genus (OTU 553961) and
3 *Pseudomonadaceae* family (OUT 543958) were introduced from surrounding seawater into the
4 mesocosm bags. Assuming the bacterioplankton concentration at day 2 representing the concentration
5 of *Pseudomonadaceae*, one of the most abundant bacterioplankton groups from surrounding seawater,
6 the concentration of *Pseudomonadaceae* at day 1 could be estimated based on the growth rate (μ_{\max}
7 $h^{-1}=0.75$) of *Pseudomonas aeruginosa* reported in (Adav and Lee, 2008) and the bacterioplankton
8 concentration at day 2. The estimated concentration of *Pseudomonadaceae* at day 1 was 101.93 cells/ml.
9 Therefore, the ratio of bacteria being continuously introduced to actual standing stocks in the
10 mesocosms was low, which allowed us to detect potential CO₂ effects in this mesocosm experiment.

11 The seawater used in this mesocosm experiment was filtered natural seawater (through 0.01 μm filter)
12 in Wuyuan bay. Although no bacteria or phytoplankton were detected in the filtered seawater by flow
13 cytometry, high concentrations of DOM (dissolved organic matter) and other nutrients in the seawater
14 could not be filtered out. According to Yan Li et al (unpublished), the dissolved organic carbon (DOC)
15 concentration was 258.9 $\mu\text{mol/ml}$ in average at day 2. It was not surprising that bacterioplankton were
16 able to grow very quickly with such high concentrations of DOC. Because the
17 phytoplankton-associated bacterioplankton were presumably adapted to the phytoplankton cultures,
18 they were used to living in the artificial seawater, not the local seawater in Wuyuan Bay. As the local
19 bacterioplankton were presumably well adapted to local conditions (such as high DOC concentration)
20 in Wuyuan Bay, it is perhaps not surprising that they could easily outcompete the phytoplankton
21 culture-derived bacterioplankton. Although bacterioplankton from the phytoplankton cultures were
22 inoculated into the mesocosm system at the beginning of the experiment, they were mostly replaced by

1 the natural bacterioplankton community within several days. Therefore, the natural bacterioplankton,
2 not the original bacterioplankton from the phytoplankton culture, mainly determined the final responses
3 of the community to different CO₂ concentrations.

4 In this mesocosm experiment, significant variation in community structure was observed through the
5 whole diatom bloom process, suggesting that the diatom bloom was a major driver for bacterioplankton
6 community structure dynamics in both the HC and LC treatments. This finding is in line with previous
7 mesocosm experiments and field observations (Allgaier et al., 2008, Teeling et al., 2012). Along with
8 the phytoplankton bloom process, the inter-replicate variation of bacterioplankton community became
9 more apparent, which was inevitable for an outdoor mesocosm experiment. For example, the
10 bacterioplankton community in mesocosm bag 8 was dominated by *Phaeobacter. sp* at day 29, which
11 was distinct from the other mesocosm bags. According to the phytoplankton data mesocosm bag 8 was
12 probably contaminated with dinoflagellates at a late stage of the algal bloom, likely resulting in a
13 different bacterioplankton community structure compared to the others. In general, no statistically
14 significant differences were detected in this study, probably due to high variability among replicates. At
15 day 10 the inter-replicate-variability in the relative abundance of some groups of bacterioplankton was
16 relatively low, especially for the HC treatment. Indeed, statistically significant differences between the
17 HC and LC treatments in the abundances of certain groups of bacterioplankton were detected at day 10.
18 Therefore, only when the variability among replicates was smaller than the variability between
19 different treatments could statistically differences between treatments be detected.

20 Although effects of elevated CO₂ on bacterioplankton communities have been reported (Allgaier et al.,
21 2008; Tanaka et al., 2008; Wang et al., 2016; Zhang et al., 2013; Ray et al., 2012; Roy et al., 2013;
22 Baltar et al., 2015; reviewed in Hutchins and Fu, 2017), how marine bacteria communities react to the

1 occurrence of elevated CO₂ in eutrophic seawater is still uncertain. This mesocosm study
2 comprehensively investigated the effects of elevated CO₂ on bacterioplankton community structure and
3 networks using Illumina sequencing and ecological network analysis in the context of eutrophication.
4 Compared to the effects of the phytoplankton bloom, ocean acidification did not strongly influence the
5 bacterioplankton community structure. The results indicate that bacterial abundance and community
6 structure at different taxonomic levels were generally similar between the HC and LC treatments at the
7 different diatom bloom stages, in line with previous ocean acidification mesocosm bacterioplankton
8 community studies (Tanaka et al., 2008; Wang et al., 2016; Zhang et al., 2013; Ray et al., 2012; Roy et
9 al., 2013; Baltar et al., 2015). Differences in bacterioplankton community diversity between the HC and
10 LC treatments were also not remarkable. These results suggest the possibility that the whole
11 bacterioplankton community has a certain degree of resilience to elevated CO₂, which is consistent with
12 a previous stated hypothesis (Joint et al., 2011).

13 It has previously been proposed that the observed insignificant effects of ocean acidification on coastal
14 bacterioplankton may be due to their adaptation to strong natural variability in pH in coastal ecosystems,
15 where amplitudes of >0.3 units from diel fluctuations and seasonal dynamics are commonly seen
16 (Hofmann et al., 2011). The comparative ecological network analysis in this study to some extent
17 explains the resilience of the bacterioplankton community to elevated CO₂ levels. According to the
18 present study, substantial numbers of OTUs that were sparsely distributed in different and small modules
19 in the LC network became connected with each other and formed fewer modules in the HC network,
20 implying elevated CO₂ has the potential to reassemble the bacterioplankton community (Fig. 4). The
21 positive relationship among these principal components were almost unaltered in the network analysis,
22 suggesting that the positive relationships among them were robust in the face of CO₂ changes, thus

1 contributing to whole community stability (Fig. 4). It has also been reported that sparsely distributed
2 fungal species were reassembled into highly connected dense modules under long-term elevated CO₂
3 conditions (Tu et al., 2015).

4 It is noteworthy that the OTUs involved in possible community reassembly were not very abundant,
5 whereas the relationship between the abundant OTUs was virtually unaltered by elevated CO₂ in this
6 study. Although elevated CO₂ promoted the reassembly of the bacterioplankton community, the network
7 constructed by abundant OTUs which are usually considered as the foundation of the whole
8 bacterioplankton community was still stable in response to elevated CO₂. This to some extent led to
9 maintenance of bacterioplankton community structure under the ocean acidification stimuli in the
10 context of eutrophic conditions. Additionally, these data indicate that more negative than positive
11 relationships between OTUs were observed in both HC and LC treatments, which is consistent with a
12 previous ocean acidification mesocosm study conducted in the Arctic Ocean (Wang et al., 2016). It was
13 proposed that a community with more competitors would be more stable and yield less variation under
14 environmental fluctuations (Gonzalez and Loreau, 2009). Therefore, it could be speculated that the
15 dominant competitive relationship between bacterioplankton species in this mesocosm experiment
16 helped the whole bacterioplankton community to adapt to pH perturbations, with less variation in total
17 biomass and diversity.

18 Although the effects of elevated CO₂ on bacterioplankton community structure were not significant,
19 the proportion of some groups of bacterioplankton varied between the HC and LC treatments in the early
20 stages of the diatom bloom. Elevated CO₂ significantly increased the proportion of Flavobacteria
21 (dominated by Flavobacteriales) in the HC treatment at day 10, when the diatoms cells began to grow
22 rapidly. In contrast, the HC treatment had negative effects on the growth of Alphaproteobacteria

1 compared to the LC treatment. The results reported here are in line with previous reports about the
2 response of Flavobacteria to ocean acidification in biofilm and single species experiments (Witt et al.,
3 2011; Teira et al., 2012). Flavobacteria are considered as the “first responders” to phytoplankton blooms
4 because they specialize in attacking algal cells and further degrading biopolymers and organic matter
5 derived from algal detrital particles (Kirchman, 2002; Teeling et al., 2012). Flavobacteria are especially
6 good at converting high molecular weight (HMW) dissolved organic matter (DOM) to low molecular
7 weight (LMW) DOM using the highly efficient, extracellular, multi-protein complex TonB-dependent
8 transporter (TBDT) system, based on previous in situ proteomics and metatranscriptomics data (Teeling
9 et al., 2012). Higher abundance of Flavobacteria under elevated CO₂ means more HMW DOM could be
10 degraded and so enter into the carbon cycle (Buchan et al., 2014). Based on the results reported here, it
11 can be speculated that increased amounts of Flavobacteria under the elevated CO₂ treatment in eutrophic
12 seawater could promote the TBDT system to break down HMW DOM and lead to improved efficiency
13 of the Microbial Carbon Pump (MCP), and possibly further influence the carbon storage in the ocean
14 (Jiao et al., 2010). It has also been postulated that the Flavobacteria-originated, light-driven proton pump
15 proteorhodopsin could be involved in dealing with ocean acidification and pH perturbation (Fuhrman et
16 al., 2008). Recent metatranscriptomic data further emphasize the role of proteorhodopsin in pH
17 homeostasis in bacterioplankton under elevated CO₂ (Bunse et al., 2016; Gómez-Consarnau et al., 2007).
18 The underlying mechanisms underlying the enhanced growth of Flavobacteria under elevated CO₂ need
19 further investigation in the future.

20 Interestingly, Flavobacteria in our study showed higher abundance in the HC treatment in the early
21 phytoplankton bloom stage. However, a negative relationship between CO₂ level and relative abundance
22 of Bacteroidetes based on terminal restriction fragment length polymorphism (T-RFLP) method was

1 observed in a mesocosm experiment conducted in the Arctic region with low nutrient levels (Roy et al.,
2 2013). Moreover, the effects of elevated CO₂ on bacterioplankton community interaction webs in this
3 study were not observed in previous mesocosm work in the Arctic Ocean (Wang et al., 2016; Roy et al.,
4 2013). The results of the current study showed that the effects of elevated CO₂ in the context of
5 eutrophication were different compared to elevated CO₂ on bacterioplankton community networks in a
6 mesocosm study carried out in the oligotrophic Arctic Ocean. The data here and previously reported,
7 seemingly contradictory results highlight the importance of including the combined effects of ocean
8 acidification and other anthropogenic perturbations to interpret and predict the impact of global change
9 on marine life.

10 In this study, the majority of the particle-attached and algae-attached bacteria were filtered out by
11 sequential filtering. Additionally, the archaea were not included in our data because we used the
12 primers 341F/805R, which do not target archaea. Therefore, the community structure of
13 particle-associated bacteria and all archaea were not investigated in our study. Furthermore, a
14 simplified model phytoplankton community was used in this study, composed of the two diatom species
15 *P. tricornutum* and *T. weissflogii* in both LC and HC treatments. It is possible that the similarity of the
16 two bacterial communities in the two treatments was due to the similar composition and quality of DOM
17 produced by these two diatoms. With a more diverse natural phytoplankton community experimental
18 system, perhaps different phytoplankton taxa would have dominated in the HC and LC treatments,
19 leading to different bacterial communities. In future studies, it would also be worthwhile to sample over
20 a diel cycle in order to understand the cyclic variability in pH, and whether this affects short term changes
21 in bacterioplankton community structure.

1 **Conclusion**

2 Elevated CO₂ was not a strong influence on bacterioplankton community structure compared to the
3 diatom bloom process, based on 16S V3-V4 region Illumina sequencing. Based on ecological network
4 analysis, elevated CO₂ appeared to reassemble the community network of taxa present with low
5 abundance, but barely altered the network structure of the bacterioplankton taxa present with high
6 abundance. It is this differential sensitivity of common and rare groups to carbonate chemistry changes
7 that may largely explain the resilience of the bacterioplankton community to elevated CO₂.

8 **Author contributions**

9 Conceived and designed the experiments: K. Gao, X. Lin, M. Dai. Performed the experiments: R. Huang,
10 X. Lin, Y. Wu, Y. Li and F. Li. Analysed data: R. Huang and X. Lin. Wrote the paper: X. Lin. Revised
11 the paper: D. Hutchins and K. Gao. All authors reviewed the manuscript.

12 **Acknowledgments**

13 This study was supported by the National Key Research and Development Program of China (Grant No.
14 2016YFA0601302), the National Natural Science Foundation of China (No. 41306096 to X. Lin, No.
15 41430967 and No. 41120164007 to K. Gao), State Oceanic Administration of China
16 (SOA,GASI-03-01-02-04), The Open Fund of Key Laboratory of Marine Ecology and Environmental
17 Sciences, Institute of Oceanology, Chinese Academy of Sciences, and Laboratory of Marine Ecology
18 and Environmental Science, Qingdao National Laboratory for Marine Science and Technology
19 (KLMEES201608), Joint project of NSFC and Shandong province (Grant No. U1406403), Strategic
20 Priority Research Program of Chinese Academy of Sciences (Grant No. XDA11020302). DAH's
21 contributions were supported by U.S. NSF OCE 1260490 and 1538525, and his visits to Xiamen were

1 supported by “111” project from the Ministry of Education. We thank X. Liu, T. Xing, X. Cai, N. Liu, S.
2 Tong, X. Yi, T. Wang, H. Miao, Z. Li, D. Yan, W. Zhao and X. Zeng for their kind assistance in
3 operations of the mesocosm experiment.

4 **Competing interests:**

5 The authors declare no competing financial interests.

6 **Reference**

- 7 Allgaier, M., Riebesell, U., Vogt, M., Thyraug, R. and Grossart, H.-P.: Coupling of heterotrophic
8 bacteria to phytoplankton bloom development at different pCO₂ levels: a mesocosm study,
9 *Biogeosciences*, 5(4), 1007–1022, doi:10.5194/bgd-5-317-2008, 2008.
- 10 Anderson, M. J.: A new method for non-parametric multivariate analysis of variance, *Austral Ecol.*,
11 26(2001), 32–46, doi:10.1046/j.1442-9993.2001.01070.x, 2001.
- 12 Adav, S. S. and Lee, D. J.: Physiological characterization and interactions of isolates in
13 phenol-degrading aerobic granules, *Appl. Microbiol. Biotechnol.*, 78(5), 899–905,
14 doi:10.1007/s00253-008-1370-0, 2008.
- 15 Azam, F.: Microbial control of oceanic carbon flux: the plot thickens., *Science* (80-.), 280(5364),
16 694–696, doi:10.1126/science.280.5364.694, 1998.
- 17 Baltar, F., Palovaara, J., Vila-Costa, M., Salazar, G., Calvo, E., Pelejero, C., Marras é C., Gasol, J. M.
18 and Pinhassil, J.: Response of rare, common and abundant bacterioplankton to anthropogenic
19 perturbations in a Mediterranean coastal site, *FEMS Microbiol. Ecol.*, 91(6), 1–12,
20 doi:10.1093/femsec/fiv058, 2015.
- 21 Buchan, A., LeClerc, G. R., Gulvik, C. A. and González, J. M.: Master recyclers: features and functions

1 of bacteria associated with phytoplankton blooms, *Nat. Rev. Microbiol.*, 12(10), 686–698,
2 doi:10.1038/nrmicro3326, 2014.

3 Bunse, C., Lundin, D., Karlsson, C. M. G., Vila-Costa, M., Palovaara, J., Akram, N., Svensson, L.,
4 Holmfeldt, K., González, J. M., Calvo, E., Pelejero, C., Marrasé C., Dopson, M., Gasol, J. M. and
5 Pinhassi, J.: Response of marine bacterioplankton pH homeostasis gene expression to elevated CO₂,
6 *Nat. Clim. Chang.*, (January), doi:10.1038/nclimate2914, 2016.

7 Busch, D. S., O'Donnell, M. J., Hauri, C., Mach, K. J., Poach, M., Doney, S. C. and Signorini, S. R.:
8 Understanding, characterizing, and communicating responses to ocean acidification: Challenges and
9 uncertainties, *Oceanography*, 28(2), 30–39, doi:http://dx.doi.org/10.5670/oceanog.2015.29, 2015.

10 Cai, W.-J., Hu, X., Huang, W.-J., Murrell, M. C., Lehrter, J. C., Lohrenz, S. E., Chou, W.-C., Zhai, W.,
11 Hollibaugh, J. T., Wang, Y., Zhao, P., Guo, X., Gundersen, K., Dai, M. and Gong, G.-C.: Acidification
12 of subsurface coastal waters enhanced by eutrophication, *Nat. Geosci.*, 4(11), 766–770,
13 doi:10.1038/ngeo1297, 2011.

14 Cao, Z., Dai, M., Zheng, N., Wang, D., Li, Q., Zhai, W., Meng, F. and Gan J.: Dynamics of the
15 carbonate system in a large continental shelf system under the influence of both a river plume and
16 coastal upwelling, *Journal of Geophysical Research: Biogeosciences*, 116(G2): 582-593, doi:
17 10.1029/2010jg001596, 2011

18 Caporaso, J. G., Kuczynski, J., Stombaugh, J., Bittinger, K., Bushman, F. D., Costello, E. K., Fierer, N.,
19 Peña, A. G., Goodrich, J. K., Gordon, J. I., Huttley, G. a, Kelley, S. T., Knights, D., Koenig, J. E., Ley,
20 R. E., Lozupone, C. a, McDonald, D., Muegge, B. D., Pirrung, M., Reeder, J., Sevinsky, J. R.,
21 Turnbaugh, P. J., Walters, W. a, Widmann, J., Yatsunenko, T., Zaneveld, J. and Knight, R.:
22 correspondence QIIME allows analysis of high- throughput community sequencing data Intensity

1 normalization improves color calling in SOLiD sequencing, *Nat. Publ. Gr.*, 7(5), 335–336,
2 doi:10.1038/nmeth0510-335, 2010a.

3 Caporaso, J. G., Bittinger, K., Bushman, F. D., Desantis, T. Z., Andersen, G. L. and Knight, R.:
4 PyNAST: A flexible tool for aligning sequences to a template alignment, *Bioinformatics*, 26(2), 266–
5 267, doi:10.1093/bioinformatics/btp636, 2010b.

6 Clarke, K. R.: Non-parametric multivariate analyses of changes in community, *Aust. J. Ecol.*, 18(1),
7 117–143, doi:10.1111/j.1442-9993.1993.tb00438.x, 1993.

8 Deng, Y., Jiang, Y.-H., Yang, Y., He, Z., Luo, F. and Zhou, J.: Molecular ecological network analyses,
9 *BMC Bioinformatics*, 13, 113, doi:10.1186/1471-2105-13-113, 2012.

10 Falkowski, P. G., Fenchel, T. and Delong, E. F.: The Microbial Engines That Drive Earth's
11 Biogeochemical Cycles, *Science* (80-.), 320(5879), 1034–1039, doi:10.1126/science.1153213, 2008.

12 Francis, C. A., Roberts, K. J., Beman, J. M., Santoro, A. E. and Oakley, B. B.: Ubiquity and diversity
13 of ammonia-oxidizing archaea in water columns and sediments of the ocean, , 102(41), 14683–14688,
14 doi:10.1073/pnas.0506625102, 2005.

15 Fuhrman, J. a, Schwalbach, M. S. and Stingl, U.: Proteorhodopsins: an array of physiological roles?,
16 *Nat. Rev. Microbiol.*, 6(6), 488–494, doi:10.1038/nrmicro1893, 2008.

17 Gattuso, J.-P., Magnan, A., Bille, R., Cheung, W. W. L., Howes, E. L., Joos, F., Allemand, D., Bopp,
18 L., Cooley, S. R., Eakin, C. M., Hoegh-Guldberg, O., Kelly, R. P., Portner, H.-O., Rogers, a. D.,
19 Baxter, J. M., Laffoley, D., Osborn, D., Rankovic, A., Rochette, J., Sumaila, U. R., Treyer, S. and
20 Turley, C.: Contrasting futures for ocean and society from different anthropogenic CO2 emissions
21 scenarios, *Science* (80-.), 349(6243), aac4722-1-aac4722-10, doi:10.1126/science.aac4722, 2015.

22 G ómez-Consarnau, L., Gonz ález, J. M., Coll-Llad ó, M., Gourdon, P., Pascher, T., Neutze, R.,

1 Pedrós-Alió, C. and Pinhassi, J.: Light stimulates growth of proteorhodopsin-containing marine
2 Flavobacteria, *Nature*, 445(7124), 210–213, doi:10.1038/nature05381, 2007.

3 Gonzalez, A. and Loreau, M.: The Causes and Consequences of Compensatory Dynamics in Ecological
4 Communities, *Annu. Rev. Ecol. Evol. Syst.*, 40(1), 393–414,
5 doi:10.1146/annurev.ecolsys.39.110707.173349, 2009.

6 Guidi, L., Chaffron, S., Bittner, L., Eveillard, D., Larhlimi, A., Roux, S., Darzi, Y., Audic, S., Berline,
7 L., Brum, J., Coelho, L. P., Espinoza, J. C. I., Malviya, S., Sunagawa, S., Dimier, C., Kandels-Lewis, S.,
8 Picheral, M., Poulain, J., Searson, S., Coordinators, T. O., Stemmann, L., Not, F., Hingamp, P., Speich,
9 S., Follows, M., Karp-Boss, L., Boss, E., Ogata, H., Pesant, S., Weissenbach, J., Wincker, P., Acinas, S.
10 G., Bork, P., de Vargas, C., Iudicone, D., Sullivan, M. B., Raes, J., Karsenti, E., Bowler, C. and Gorsky,
11 G.: Plankton networks driving carbon export in the oligotrophic ocean, *Nature*, 532(7600),
12 doi:10.1038/nature16942, 2016.

13 Hofmann, G. E., Smith, J. E., Johnson, K. S., Send, U., Levin, L. A., Micheli, F., Paytan, A., Price, N.
14 N., Peterson, B., Takeshita, Y., Matson, P. G., Crook, E. D., Kroeker, K. J., Gambi, M. C., Rivest, E. B.,
15 Frieder, C. A., Yu, P. C. and Martz, T. R.: High-Frequency Dynamics of Ocean pH: A
16 Multi-Ecosystem Comparison, *PLoS One*, 6(12), e28983, doi:10.1371/journal.pone.0028983, 2011.

17 Hutchins, D. A. and Fu, F.: Microorganisms and ocean global change, *Nat. Microbiol.*, 2(6), 17058,
18 doi:10.1038/nmicrobiol.2017.58, 2017.

19 Jiao, N., Herndl, G. J., Hansell, D. A., Benner, R., Kattner, G., Wilhelm, S. W., Kirchman, D. L.,
20 Weinbauer, M. G., Luo, T., Chen, F. and Azam, F.: Microbial production of recalcitrant dissolved
21 organic matter: long-term carbon storage in the global ocean, *Nat. Rev. Microbiol.*, 8(8), 593–599,
22 doi:10.1038/nrmicro2386, 2010.

1 Jin, P., Wang, T., Liu, N., Dupont, S., Beardall, J., Boyd, P. W., Riebesell, U. and Gao, K.: Ocean
2 acidification increases the accumulation of toxic phenolic compounds across trophic levels., *Nat.*
3 *Commun.*, 6(October), 8714, doi:10.1038/ncomms9714, 2015.

4 Joint, I., Doney, S. C. and Karl, D. M.: Will ocean acidification affect marine microbes?, *ISME J.*, 5(1),
5 1–7, doi:10.1038/ismej.2010.79, 2011.

6 Kirchman, D. L.: The ecology of Cytophaga-Flavobacteria in aquatic environments, *FEMS Microbiol.*
7 *Ecol.*, 39(2), 91–100, doi:10.1016/S0168-6496(01)00206-9, 2002.

8 Krause, E., Wichels, A., Giménez, L., Lunau, M., Schilhabel, M. B. and Gerdt, G.: Small Changes in
9 pH Have Direct Effects on Marine Bacterial Community Composition: A Microcosm Approach, *PLoS*
10 *One*, 7(10), e47035, doi:10.1371/journal.pone.0047035, 2012.

11 Labare, M. P., Bays, J. T., Butkus, M. a., Snyder-Leiby, T., Smith, A., Goldstein, A., Schwartz, J. D.,
12 Wilson, K. C., Ginter, M. R., Bare, E. a., Watts, R. E., Michealson, E., Miller, N. and LaBranche, R.:
13 The effects of elevated carbon dioxide levels on a *Vibrio* sp. isolated from the deep-sea, *Environ. Sci.*
14 *Pollut. Res.*, 17(4), 1009–1015, doi:10.1007/s11356-010-0297-z, 2010.

15 Langille, M., Zaneveld, J., Caporaso, J. G., McDonald, D., Knights, D., Reyes, J., Clemente, J.,
16 Burkepille, D., Vega Thurber, R., Knight, R., Beiko, R. and Huttenhower, C.: Predictive functional
17 profiling of microbial communities using 16S rRNA marker gene sequences., *Nat. Biotechnol.*, 31(9),
18 814–21, doi:10.1038/nbt.2676, 2013.

19 Lidbury, I., Johnson, V., Hall-spencer, J. M., Munn, C. B. and Cunliffe, M.: Community-level response
20 of coastal microbial biofilms to ocean acidification in a natural carbon dioxide vent ecosystem, *Mar.*
21 *Pollut. Bull.*, 64(5), 1063–1066, doi:10.1016/j.marpolbul.2012.02.011, 2012.

22 Lima-Mendez, G., Faust, K., Henry, N., Decelle, J., Colin, S., Carcillo, F., Chaffron, S.,

1 Ignacio-Espinosa, J. C., Roux, S., Vincent, F., Bittner, L., Darzi, Y., Wang, J., Audic, S., Berline, L.,
2 Bontempi, G., Cabello, A. M., Coppola, L., Cornejo-Castillo, F. M., D'Ovidio, F., De Meester, L.,
3 Ferrera, I., Garet-Delmas, M.-J., Guidi, L., Lara, E., Pesant, S., Royo-Llonch, M., Salazar, G., Sanchez,
4 P., Sebastian, M., Souffreau, C., Dimier, C., Picheral, M., Searson, S., Kandels-Lewis, S., Gorsky, G.,
5 Not, F., Ogata, H., Speich, S., Stemmann, L., Weissenbach, J., Wincker, P., Acinas, S. G., Sunagawa,
6 S., Bork, P., Sullivan, M. B., Karsenti, E., Bowler, C., de Vargas, C. and Raes, J.: Determinants of
7 community structure in the global plankton interactome, *Science* (80-.), 348(6237), 1262073–1262073,
8 doi:10.1126/science.1262073, 2015.

9 Liu, J., Weinbauer, M., Maier, C., Dai, M. and Gattuso, J.: Effect of ocean acidification on microbial
10 diversity and on microbe-driven biogeochemistry and ecosystem functioning, *Aquat. Microb. Ecol.*,
11 61(3), 291–305, doi:10.3354/ame01446, 2010.

12 Liu, N., Tong, S., Yi, X., Li, Y., Li, Z., Miao, H., Wang, T., Li, F., Yan, D., Huang, R., Wu, Y.,
13 Hutchins, D. A., Beardall, J., Dai, M. and Gao, K.: Carbon assimilation and losses during an ocean
14 acidification mesocosm experiment, with special reference to algal blooms, *Mar. Environ. Res.*, 129,
15 229–235, doi:10.1016/j.marenvres.2017.05.003, 2017.

16 McDonald, D., Price, M. N., Goodrich, J., Nawrocki, E. P., DeSantis, T. Z., Probst, A., Andersen, G. L.,
17 Knight, R. and Hugenholtz, P.: An improved Greengenes taxonomy with explicit ranks for ecological
18 and evolutionary analyses of bacteria and archaea, *ISME J.*, 6(3), 610–618,
19 doi:10.1038/ismej.2011.139, 2012.

20 Meron, D., Atias, E., Iasur Kruh, L., Elifantz, H., Minz, D., Fine, M. and Banin, E.: The impact of
21 reduced pH on the microbial community of the coral *Acropora eurystroma*, *ISME J.*, 5(1), 51–60,
22 doi:10.1038/ismej.2010.102, 2011.

1 Mielke, P. W., Berry, K. J., Brockwell, P. J. & Williams, J. S.: A class of nonparametric tests based on
2 multiresponse permutation procedures, *Biometrika*, 68(3), 720–724, 1981.

3 Ramaiah, N., Sarma, V. V. S. S., Gauns, M., Dileep Kumar, M. and Madhupratap, M.: Abundance and
4 relationship of bacteria with transparent exopolymer particles during the 1996 summer monsoon in the
5 Arabian Sea, *Proc. Indian Acad. Sci. Earth Planet. Sci.*, 109(4), 443–451, doi:10.1007/bf02708332,
6 2000.

7 Ray, J. L., Töpper, B., An, S., Silyakova, A., Spindelböck, J., Thyrraug, R., Dubow, M. S., Thingstad,
8 T. F. and Sandaa, R. A.: Effect of increased pCO₂ on bacterial assemblage shifts in response to glucose
9 addition in Fram Strait seawater mesocosms, *FEMS Microbiol. Ecol.*, 82(3), 713–723,
10 doi:10.1111/j.1574-6941.2012.01443.x, 2012.

11 Roy, A.-S., Gibbons, S. M., Schunck, H., Owens, S., Caporaso, J. G., Sperling, M., Nissimov, J. I.,
12 Romac, S., Bittner, L., Mühlhng, M., Riebesell, U., LaRoche, J. and Gilbert, J. a.: Ocean acidification
13 shows negligible impacts on high-latitude bacterial community structure in coastal pelagic mesocosms,
14 *Biogeosciences*, 10(1), 555–566, doi:10.5194/bg-10-555-2013, 2013.

15 Sugimoto, K., Fukuda, H., Baki, M. A. and Koike, I.: Bacterial contributions to formation of
16 transparent exopolymer particles (TEP) and seasonal trends in coastal waters of Sagami Bay, Japan,
17 *Aquat. Microb. Ecol.*, 46(1), 31–41, doi:10.3354/ame046031, 2007.

18 Tanaka, T., Thingstad, T. F., Løvdal, T., Grossart, H.-P., Larsen, A., Schulz, K. G. and Riebesell, U.:
19 Availability of phosphate for phytoplankton and bacteria and of labile organic carbon for bacteria at
20 different pCO₂ levels in a mesocosm study, *Biogeosciences*, (5), 669–678,
21 doi:10.5194/bgd-4-3937-2007, 2007.

22 Teeling, H., Fuchs, B. M., Becher, D., Klockow, C., Gardebrecht, A., Bennis, C. M., Kassabgy, M.,

1 Huang, S., Mann, A. J., Waldmann, J., Weber, M., Klindworth, A., Otto, A., Lange, J., Bernhardt, J.,
2 Reinsch, C., Hecker, M., Peplies, J., Bockelmann, F. D., Callies, U., Gerds, G., Wichels, A., Wiltshire,
3 K. H., Glockner, F. O., Schweder, T. and Amann, R.: Substrate-Controlled Succession of Marine
4 Bacterioplankton Populations Induced by a Phytoplankton Bloom, *Science* (80-.), 336(6081), 608–
5 611, doi:10.1126/science.1218344, 2012.

6 Teira, E., Fernández, A., Álvarez-Salgado, X. A., García-Martín, E. E., Serret, P. and Sobrino, C.:
7 Response of two marine bacterial isolates to high CO₂ concentration, *Mar. Ecol. Prog. Ser.*, 453, 27–
8 36, doi:10.3354/meps09644, 2012.

9 Tu, Q., Yuan, M., He, Z., Deng, Y., Xue, K., Wu, L., Hobbie, S. E., Reich, P. B. and Zhou, J.: Fungal
10 Communities Respond to Long-Term CO₂ Elevation by Community Reassembly, *Appl. Environ.*
11 *Microbiol.*, 81(7), 2445–2454, doi:10.1128/AEM.04040-14, 2015.

12 Wang, Y., Zhang, R., Zheng, Q., Deng, Y., Van Nostrand, J. D., Zhou, J. and Jiao, N.:
13 Bacterioplankton community resilience to ocean acidification: evidence from microbial network
14 analysis, *ICES J. Mar. Sci.*, 73(3), 865–875, doi:10.1093/icesjms/fst176, 2016.

15 Witt, V., Wild, C., Anthony, K. R. N., Diaz-Pulido, G. and Uthicke, S.: Effects of ocean acidification
16 on microbial community composition of, and oxygen fluxes through, biofilms from the Great Barrier
17 Reef, *Environ. Microbiol.*, 13(11), 2976–2989, doi:10.1111/j.1462-2920.2011.02571.x, 2011.

18 Zhang, J., Kobert, K., Flouri, T. and Stamatakis, A.: PEAR: a fast and accurate Illumina Paired-End
19 reAd mergeR, *Bioinformatics*, 30(5), 614–620, doi:10.1093/bioinformatics/btt593, 2014.

20 Zhang, R., Xia, X., Lau, S. C. K., Motegi, C., Weinbauer, M. G. and Jiao, N.: Response of
21 bacterioplankton community structure to an artificial gradient of pCO₂ in the Arctic Ocean,
22 *Biogeosciences*, 10(6), 3679–3689, doi:10.5194/bg-10-3679-2013, 2013.

1 Zhou, J., Deng, Y., Luo, F., He, Z., Tu, Q. and Zhi, X.: Functional molecular ecological networks,

2 MBio, 1(4), e00169-10, doi:10.1128/mBio.00169-10.Editor, 2010.

3

4

5

6

7

8

9

10

11

12

13

14

15

16

17

18

19

20

21

22

1 **Figure legends**

2 **Figure 1** Temporal variations of $p\text{CO}_2$ (a), pH_{NBS} (b) and $\text{Chl}a$ (c) during the whole experiment. The
3 $p\text{CO}_2$ was calculated from DIC and pH using the CO2SYS program. Data are the means \pm SD, $n=3$.

4

5 **Figure 2** Bacterioplankton community structure overview at different taxonomic levels during days 4, 6,
6 8, 10, 13, 19 and 29 (#1, #6, #8) under LC and HC (#2, #4, #7). X-axis represents sample name (for
7 example, D4.1 refers to bacterioplankton in mesocosm bag 1 collected at day 4) and the Y-axis
8 represents relative abundance of different groups of bacterioplankton.

9

10 **Figure 3** The relative abundance over time of primary taxa of the bacterioplankton community; HC in
11 red and LC in black. Proteobacteria (a) and Bacteroidetes (b) are phylum level; Flavobacteria (c) and
12 Alphabacteria (d) are class level; Flavobacteriales (e) and Rhodobacteriales (f) are order level;
13 Flavobacteriaceae (g) and Rhodobacteraceae (h) are family level. Data are the means \pm SD ($n=3$), and the
14 asterisk represents a difference at $p < 0.05$.

15

16 **Figure 4** Bacterioplankton network interactions under LC (a) and HC (b) conditions. Each node
17 represents an OTU. Node colors demonstrate different taxon. Each line connects two OTUs. A blue line
18 indicates a negative interaction between nodes, suggesting predation or competition, while a red line
19 indicates a positive interaction suggesting mutualism or cooperation. OTUs with importance are marked
20 with OTU identification numbers.

21

22 **Figure 5** Sub-modules in ecological network analysis under LC (a) and HC (b) conditions. Each dot

1 represents an OTU. The Z - P plot shows OTU distribution based on their module-based topological role
2 according to within-module (Z) and among-module (P) connectivity. The nodes were defined as module
3 hubs with $Z_i > 2.5$ and $P_i < 0.625$, which were more closely connected within the module, while the
4 connectors were nodes with $Z_i < 2.5$ and $P_i > 0.625$ were more closely connected to nodes in other
5 modules. Network hubs are super-generalist with a $Z_i > 2.5$ and $P_i > 0.625$. The other nodes were
6 considered peripheral.

7

8

9

10

11

12

13

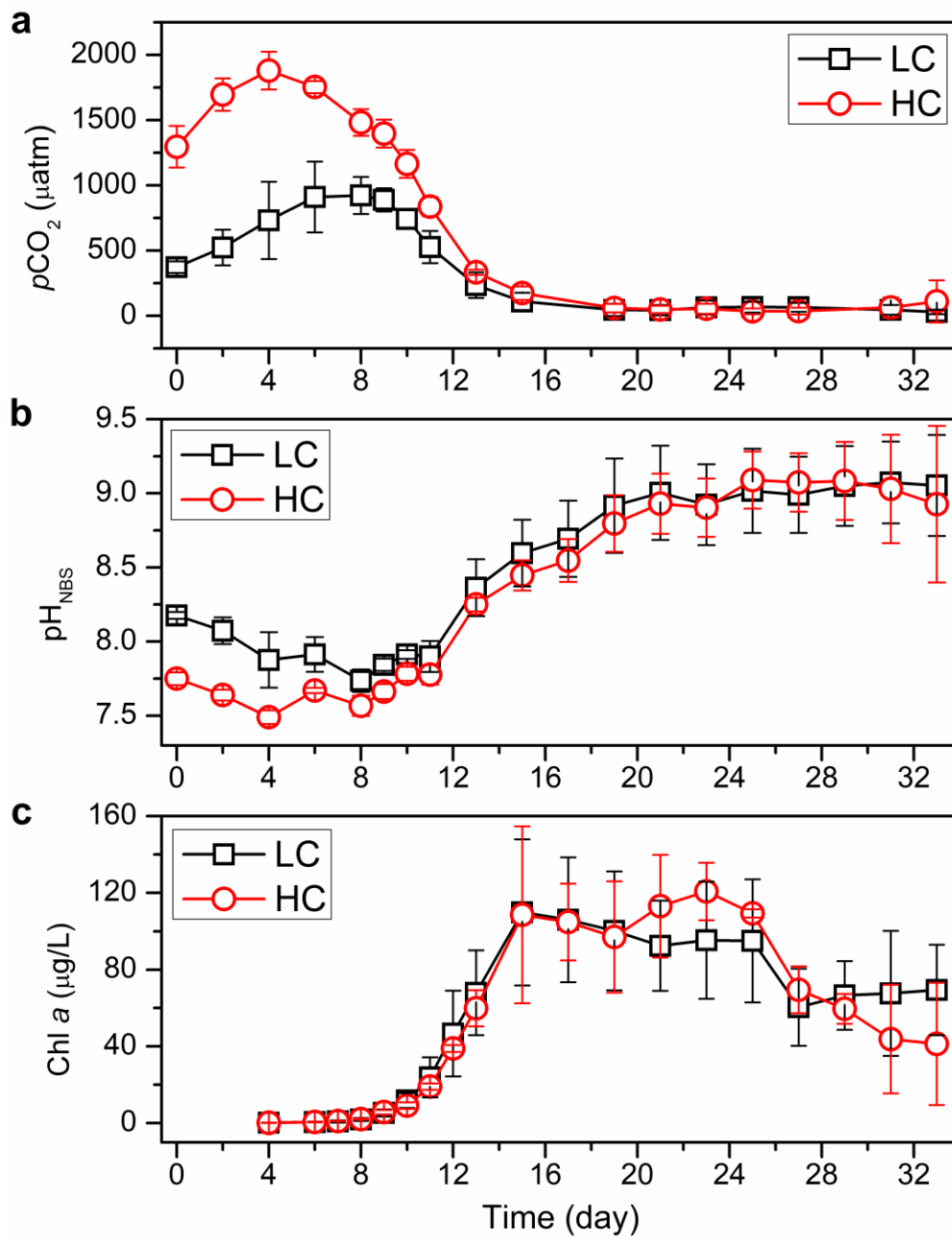
14

15

16

17

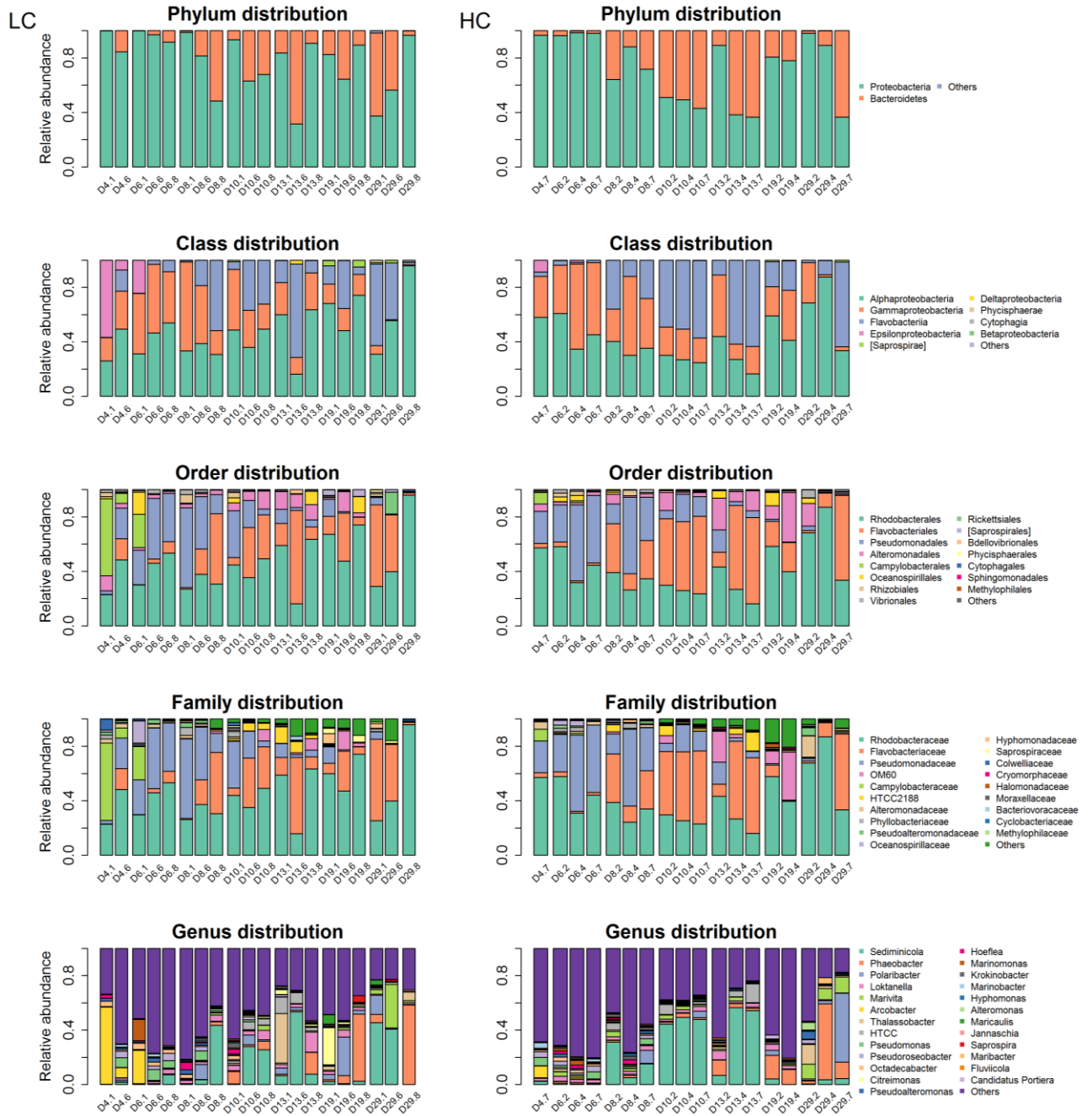
18



1

2

Figure 1



1

2

Figure 2

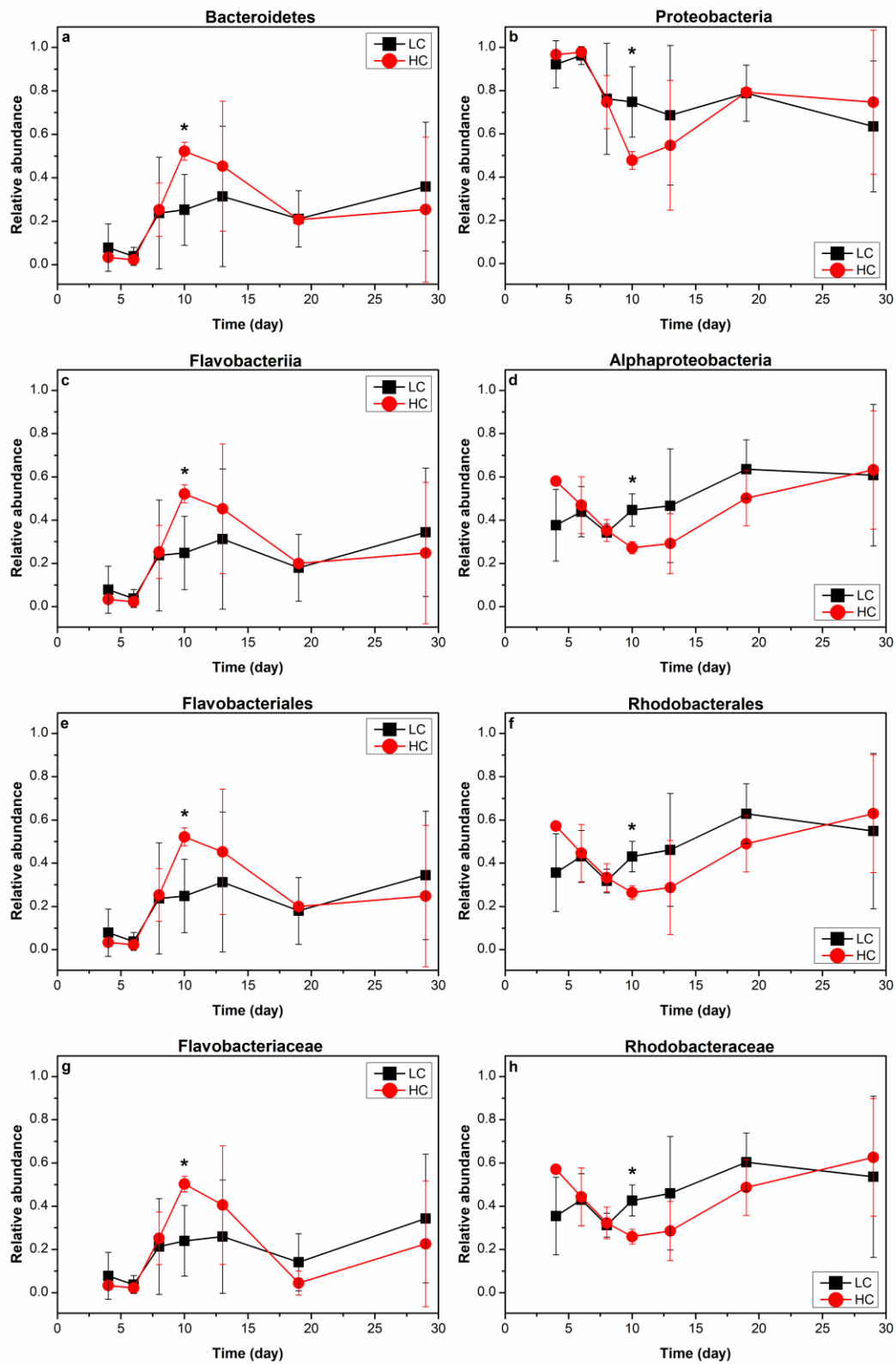


Figure 3

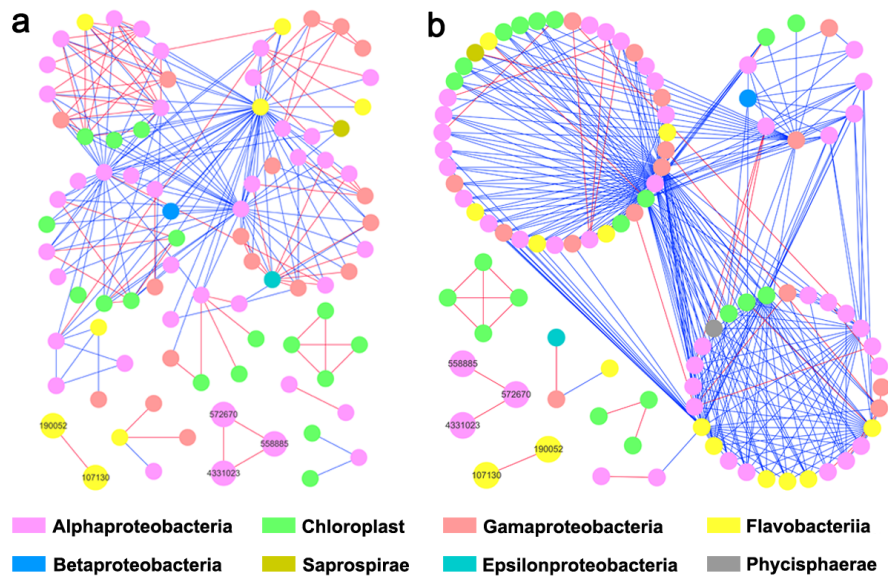


Figure 4

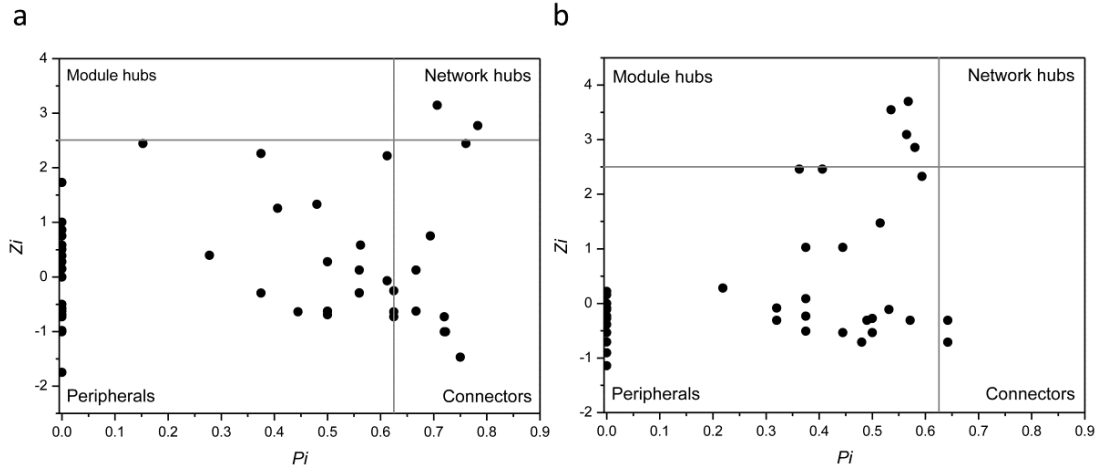


Figure 5

Table 1 Topological properties of the bacterioplankton communities as represented by molecular networks under HC and LC treatments; also their rewired random networks.

| | Experimental network | | | | | | Random network | | | |
|-----------|----------------------|-------------|-----------------|--|----------------------|---------------------------------|----------------|--|---------------------------------|-----------------|
| | Total nodes | Total links | R2 of power-law | Average clustering coefficient (avgCC) | Average connectivity | Harmonic geodesic distance (HD) | Modularity | Average clustering coefficient (avgCC) | Harmonic geodesic distance (HD) | Modularity |
| LC | 85 | 209 | 0.817 | 0.402 | 0.625 | 3.397 | 0.414 | 0.424 +/- 0.023 | 2.187 +/- 0.049 | 0.249 +/- 0.010 |
| HC | 96 | 310 | 0.817 | 0.448 | 0.714 | 2.956 | 0.303 | 0.292 +/- 0.023 | 2.306 +/- 0.059 | 0.323 +/- 0.008 |

Table 2 Dissimilarity tests of bacterial communities in the HC and LC treatments at various time points.

| | Anosim | | MRPP | | Adonis | |
|--------------|--------|---------|----------|---------|----------------|-----|
| Time | R | P-value | δ | P-value | R ² | P |
| day6 | -0.111 | 0.602 | 0.3952 | 1 | 0.15447 | 1 |
| day8 | 0.111 | 0.284 | 0.438 | 0.6 | 0.2 | 0.5 |
| day10 | 0.037 | 0.613 | 0.4929 | 0.7 | 0.17829 | 0.7 |
| day13 | 0.111 | 0.309 | 0.412 | 0.5 | 0.19714 | 0.5 |
| day19 | 0 | 0.693 | 0.4336 | 0.3 | 0.28263 | 0.3 |
| day29 | -0.259 | 1 | 0.4513 | 0.9 | 0.15517 | 0.9 |